

Enhanced magnetism in amorphous Co-Y alloys: An *ab initio* approach

D. Spišák

*Institut für Theoretische Physik, Technische Universität Wien, Wiedner Hauptstraße 8-10, A-1040 Wien, Austria
and Department of Experimental Physics, Šafárik University, Park Angelinum 9, SK 04154 Košice, Slovakia*

Ch. Becker and J. Hafner

*Institut für Theoretische Physik, Technische Universität Wien, Wiedner Hauptstraße 8-10, A-1040 Wien, Austria
(Received 26 August 1994)*

The magnetic properties of Co-Y crystalline intermetallic compounds and amorphous alloys have been investigated using molecular-dynamics simulations of the amorphous structure (based on effective tight-binding-bond forces) and self-consistent spin-polarized electronic-structure calculations (using the supercell approximation for the amorphous phases). We find that the amorphous structure is characterized by a rather strong chemical short-range order (stronger than in amorphous Fe-Y, but weaker than in Ni-Y alloys). As a consequence, the total electronic density of states (DOS) is also similar in the crystalline and amorphous phases, apart from a smearing of the fine-structure characteristic for the long-range order in the intermetallic compounds. All crystalline $\text{Co}_x\text{Y}_{100-x}$ alloys with $x \geq 75$ and all amorphous alloys with $x \geq 45$ are ferrimagnetic. The Laves phase Co_2Y shows metamagnetism. The disorder-induced smearing of the electronic DOS eliminates the metamagnetic instability and is responsible for the increase of the paramagnetic DOS at the Fermi level and for the enhancement of magnetism. We find that the ferrimagnetic coupling, together with the strong tendency to heterocoordination is important for the persistence of magnetic ordering in the Y-rich regime.

I. INTRODUCTION

A large number of experimental investigations¹⁻⁴ has established that the absence of translational symmetry affects the magnetic properties of amorphous alloys of Fe, Co, and Ni with early transition metals or rare-earth metals in various ways that are still not completely understood. Alloys of Ni with metals such as Zr or Y are ferromagnetic^{5,6} only at Ni concentrations of $x \geq 85$ at.%, and this correlates well with the enhanced paramagnetism of crystalline Ni_5Zr and the weak ferromagnetism of Ni_{17}Y_2 . Co-based alloys generally show an enhancement of the magnetic moments in the amorphous state relative to the crystalline reference compounds, and the ferromagnetism extends to lower Co concentrations in the glassy alloys.^{6,7} In Fe-based alloys with Fe concentrations of $x \leq 85$ at.% the magnetic moments are very similar in the crystalline and amorphous phases, but in the Fe-rich limit competing ferro- and antiferromagnetic exchange interactions lead to a strong reduction of the average magnetic moments and to the formation of complex noncollinear (spero- and asperomagnetic) spin structures.^{8,9} Because of the itinerant character of 3d magnetism, the magnetic properties of the amorphous transition-metal alloys are strongly dependent on the atomic short-range order. For an understanding of amorphous magnetism it is hence necessary to connect the atomic structure to the magnetic properties via the electronic structure. For the Fe-based alloys we have shown that a molecular-dynamics simulation of the atomic structure based on tight-binding-bond potentials

combined with self-consistent electronic-structure calculations in the local-spin-density approximation represents such a microscopic theory. It was shown that over a wide range of compositions both the atomic and the electronic structures are very similar in the amorphous and crystalline Fe-Zr (Ref. 10), Fe-Y (Ref. 11), and Fe-B (Ref. 12) phases, and this implies the similarity of the magnetic properties. Significant differences appear in the Fe-rich limit where short-range fluctuations in the local atomic environment lead to a competition between ferro- and antiferromagnetic exchange interactions and the formation of negative Fe moments. The interactions causing the appearance of negative moments are very sensitive to local self-consistency, therefore these effects cannot adequately be described on the basis of non-self-consistent calculations. For Co-Zr alloys similar calculations predict the onset of magnetic ordering at a composition of $x \sim 50$ at.% Co, whereas crystalline Co_2Zr is on the limit between ferro- and paramagnetism, with a small moment of $\mu_{\text{Co}} \simeq 0.0-0.16\mu_B$, depending on density. Experimentally, the formation of a ferromagnetic moment is observed on substitution of a small percentage of Co by Fe. However, the influence of the structural disorder on the magnetic properties cannot be studied in detail, because the Laves-phase Co_2Zr is the only stable Co-rich intermetallic compound. The situation is different for Co-Y alloys where the existence of a number of stable intermetallic compounds (Co_{17}Y_2 , Co_5Y , Co_{23}Y_6 , Co_7Y_2 , Co_3Y , Co_2Y , CoY , Co_3Y_4 , Co_5Y_8 , CoY_3) allows for a very detailed investigation. In the literature, several attempts have been made to solve this prob-

lem. Moruzzi *et al.*¹³ proposed (on the basis of spin-polarized electronic structure calculations for Co_3Y , but in a Cu_3Au -type model structure and not in the real Be_3Nb structure) that a volume-induced magnetic instability occurs in Co_xY , $x = 2-3$, with the crystalline and amorphous phases lying on either side of the instability. The existence of a magnetic instability is corroborated by the results of Mohn and Schwarz¹⁴ who showed that for crystalline Co_2Y a paramagnetic solution coexists with a ferromagnetic solution over a wide range of densities. At the theoretical equilibrium density, the paramagnetic solution is lower in energy, whereas at the experimental density the ferromagnetic state is stable. On the other hand, Buschow,⁷ Inoue and Shimizu,¹⁵ and most recently Kakehashi and Yu¹⁶ have argued that the enhancement of magnetism is due to a decrease of the chemical short-range order (CSRO) in the amorphous relative to the crystalline intermetallic compounds leading to a stronger Co-Co interaction at the expense of a weaker Co-Y coupling. However, this argument too is not unproblematic: detailed neutron-diffraction investigations [using isotopic substitution¹⁷ for the determination of the partial correlation functions of $\text{Ni}_x\text{Y}_{100-x}$, and isomorphic substitution¹⁸ for $(\text{Fe}_y\text{Mn}_{100-y})_x\text{Y}_{100-x}$] have demonstrated that the degree of CSRO is very high in $\alpha\text{-Ni}_x\text{Y}_{100-x}$ and still appreciable for $\alpha\text{-Fe}_x\text{Y}_{100-x}$. This has also been confirmed by detailed molecular-dynamics (MD) modeling studies.¹⁹ Less is known about the structure of $\alpha\text{-Co}_x\text{Y}_{100-x}$, but from the results on the Ni and Fe alloys we have to expect a considerable degree of CSRO in these alloys as well. What appears to be necessary is to perform a calculation which determines the details of the atomic structure in a way that is consistent with what is known about the electronic structure (instead of postulating *a priori* maximum chemical disorder for the amorphous phase), and to base the investigation of the magnetic properties on this realistic model structure. Such an investigation is the subject of the present paper. We report detailed molecular-dynamics studies of the atomic structure and self-consistent spin-polarized electronic-structure calculations for crystalline and amorphous Co-Y alloys that show that a very accurate prediction of the magnetic properties of all phases can be achieved.

II. ATOMIC STRUCTURE

The atomic structure of the amorphous alloys has been calculated by a simulated molecular-dynamics quench, based on interatomic forces from the hybridized nearly-free-electron tight-binding-bond (NFE-TBB) theory.^{11,20} The theory of the interatomic interactions is well documented in our papers in a series of Ni-based alloys (including Ni-Y),²⁰ $\alpha\text{-Fe-Y}$ (Ref. 11), and amorphous Fe-metalloid alloys,²¹ we also refer to those papers concerning all technical details of the MD simulations. In particular, it has been shown that the MD simulations performed for Ni-Y and Fe-Y using the NFE-TBB potentials reproduce not only the partial structure factors measured by neutron-scattering and isotopic, respectively, isomor-

phic substitution,¹⁷ they also describe the small-angle scattering intensities and hence the medium-range order correctly. In addition, these potentials have been used to calculate the phonon spectra and dynamical structure factors of amorphous Ni-Zr (Ref. 22) and Fe-B (Ref. 23). All input data are determined for the pure metals, no fitting is necessary to construct the potentials for the alloys.

Figure 1 shows a characteristic set of interatomic potentials for the critical composition for the onset of magnetism, $\text{Co}_{67}\text{Y}_{33}$. The important features are the strong preferential Co-Y interactions (leading to a trend to heterocoordination) and the nonadditivity of the repulsive diameters causing short Co-Y bond lengths. In Co-Y these effects are stronger than in Fe-Y, but weaker than in Ni-Y, hence we expect a similar trend in the local order of the amorphous phases. Figure 2 shows the partial pair correlation functions of a selected series of amorphous $\text{Co}_x\text{Y}_{100-x}$ alloys. They reflect (a) the strong chemical order at all compositions, (b) the strong influence of the nonadditivity of the interatomic interactions on the interatomic distances [the Co-Y nearest-neighbor distances are reduced relative to the average of the Co-Co and Y-Y distances by 8.6% (in $\text{Co}_{83}\text{Y}_{17}$) to 14.9% (in $\text{Co}_{40}\text{Y}_{60}$)], and (c) a topological short range that conforms with the principles of tetrahedral close packing of a mixture of large and small atoms in the Co-rich regime, whereas in the Y-rich regime it already shows a transition to the trigonal-prismatic order characteristic for the amorphous Ni-Y and Ni-Zr alloys.²⁰ From the aspect of the composition dependence of the magnetization, the

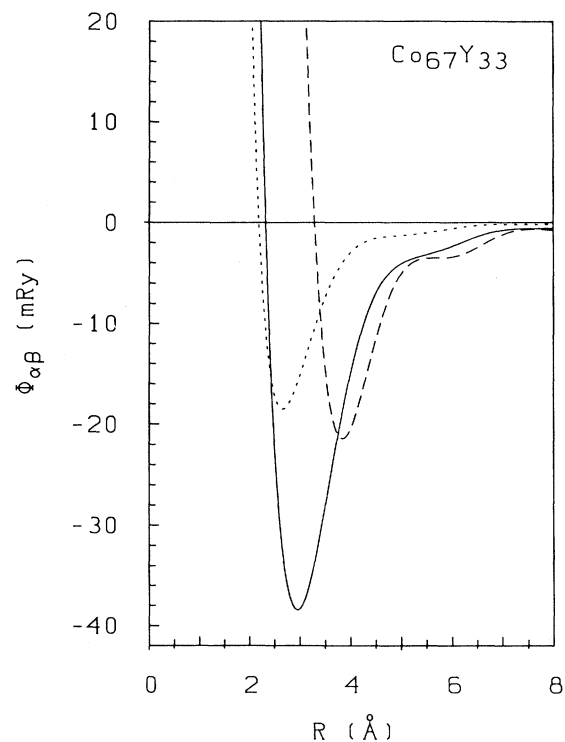


FIG. 1. Effective interatomic potentials in $\alpha\text{-Co}_{67}\text{Y}_{33}$ alloy: $\Phi_{\text{Co-Y}}$ (full line), $\Phi_{\text{Y-Y}}$ (dashed line), $\Phi_{\text{Co-Co}}$ (dotted line).

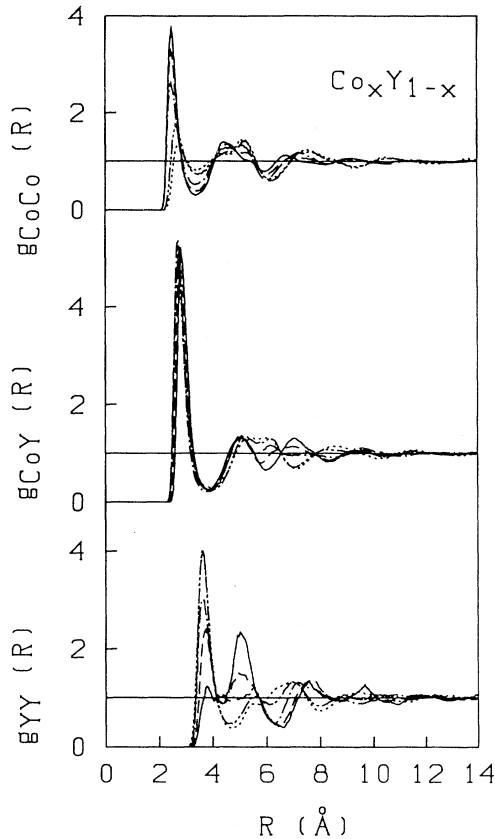


FIG. 2. Partial pair correlation functions $g_{ij}(R)$; $i, j = \text{Co, Y}$ of amorphous $\text{Co}_x\text{Y}_{100-x}$ alloys: $\text{Co}_{83}\text{Y}_{17}$ (solid line), $\text{Co}_{75}\text{Y}_{25}$ (dashed line), $\text{Co}_{67}\text{Y}_{33}$ (dot-dashed), $\text{Co}_{50}\text{Y}_{50}$ (dot-dot-dashed), $\text{Co}_{40}\text{Y}_{60}$ (dotted line).

most important aspect is the CSRO of the amorphous phases, in relation to the intermetallic compounds²⁴ and as a function of composition. The partial coordination numbers are compiled in Table I. The results confirm that the CSRO is very similar in the amorphous and in the crystalline phases—also around the composition of

the Laves-phase Co_2Y where the difference in the magnetic properties is largest. We also emphasize the strong decrease of the number of Co-Co pairs with increasing Y concentrations. This will be important for the interpretation of the physical mechanism for the formation of magnetic moments.

The amorphous structure of Co-Y is thus intermediate between that of Fe-Y and Ni-Y: the phases with a high content of the magnetic metal have a polytetrahedral local order, with a CSRO that decreases slightly in the series (Ni-Co-Fe)-Y; the Y-rich phases show a trigonal-prismatic local order that is strong in Ni-Y, weaker in Co-Y and has essentially broken down in $\text{Fe}_x\text{Y}_{100-x}$ which shows medium-range concentration fluctuations^{11,17} on the scale of 10–15 Å. No medium-range fluctuations are predicted for amorphous Co-Y.

III. ELECTRONIC STRUCTURE AND MAGNETIC PROPERTIES OF CRYSTALLINE Co-Y COMPOUNDS

For a brief characterization of the magnetic properties of the crystalline Co-Y compounds we performed spin-polarized electronic structure calculations using the linear-muffin-tin-orbital (LMTO) method²⁵ in the atomic sphere approximation for Co_5Y (CaCu₅ structure), Co_3Y (Be₃Nb structure) and Co_2Y (Cu₂Mg structure). The total and partial densities of states are given in Fig. 3. Previous electronic structure calculations had been presented by Mohn and Schwarz,¹⁴ Yamada *et al.*,²⁶ and Cyrot and Lavagna²⁷ for Co_2Y and by Coehoorn²⁸ for Co_{12}Y , Co_{17}Y_2 , Co_5Y , Co_{23}Y_6 , and Co_3Y . The crystallographic input data are compiled in Table II, for the Brillouin-zone integrations we have used the linear-tetrahedron method with grids of 225, 112, and 505 \vec{k} points in the irreducible part of the zone for Co_5Y , Co_3Y , and Co_2Y , respectively. Co_5Y and Co_3Y show the electronic density of states (DOS) characteristic for a strong ferrimagnet, with a larger bandwidth and a stronger bonding-antibonding splitting in the minority spin band.

TABLE I. Average coordination numbers in amorphous and crystalline $\text{Co}_x\text{Y}_{100-x}$ alloys.

		N_{ij}					
		Co-Co	Co-Y	Co_{tot}	Y-Co	Y-Y	Y_{tot}
$\text{Co}_{83}\text{Y}_{17}$ (amorph.) ^a		9.2	3.4	12.6	16.4	1.2	17.6
Co_5Y (CaCu ₅ struct.) ^b	CoI	9.0	3.0	12.0	18.0	2.0	20.0
	CoII	8.0	4.0	12.0			
$\text{Co}_{75}\text{Y}_{25}$ (amorph.) ^a		7.1	4.6	11.7	13.9	4.3	18.2
Co_3Y (Be ₃ Nb struct.) ^b	CoI	6.0	6.0	12.0	18.0	2.0	20.0
	CoII	9.0	3.0	12.0	12.0	4.0	16.0
	CoIII	7.0	5.0	12.0			
$\text{Co}_{67}\text{Y}_{33}$ (amorph.) ^a		5.8	5.5	11.3	11.3	7.0	18.3
Co_2Y (Cu ₂ Mg struct.) ^b		6.0	6.0	12.0	12.0	4.0	16.0
$\text{Co}_{60}\text{Y}_{40}$ (amorph.) ^a		4.3	6.3	10.6	9.4	8.9	18.3
$\text{Co}_{50}\text{Y}_{50}$ (amorph.) ^a		3.1	6.8	9.9	6.8	10.3	17.1
$\text{Co}_{40}\text{Y}_{60}$ (amorph.) ^a		1.6	7.3	8.9	4.9	11.6	16.5

^aCalculated by integrating the first peak of the partial radial distribution functions up to the first minimum.

^bCrystal structure data from Villars and Calvert (Ref. 24).

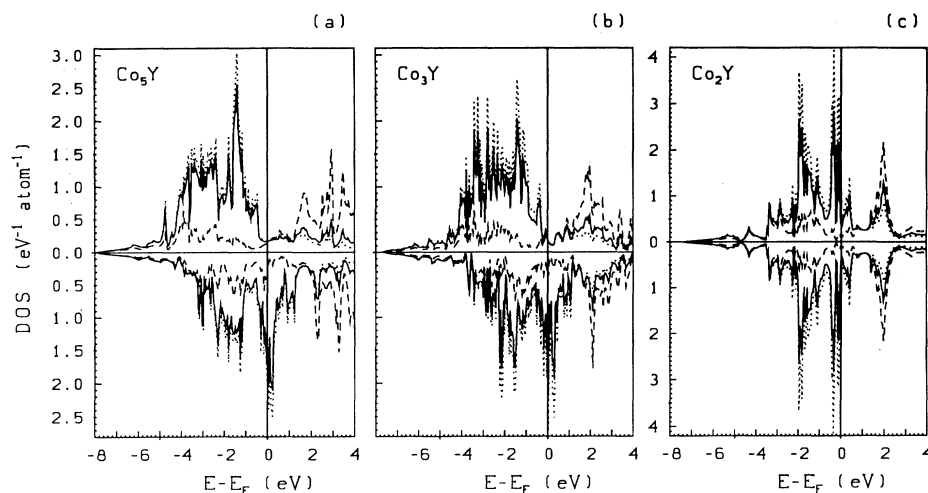


FIG. 3. Total and partial spin-polarized electronic densities of state for crystalline Co-Y compounds: total DOS (solid line), partial Y-DOS (dashed line), partial Co-DOS (dotted line). Total and partial densities of state are normalized to the same number of atoms. For Co_2Y only the paramagnetic solution is shown.

The strong covalent coupling of the Y $4d$ states to the minority-spin band of Co induces a negative Y moment. The calculated moments are $\bar{\mu}_{\text{Co}} = 1.52\mu_B$, $\mu_{\text{CoI}} = 1.46\mu_B$, $\mu_{\text{CoII}} = 1.56\mu_B$, $\mu_Y = -0.40\mu_B$, $\bar{\mu} = 1.20\mu_B$ for Co_5Y and $\bar{\mu}_{\text{Co}} = 1.34\mu_B$, $\mu_{\text{CoI}} = 1.20\mu_B$, $\mu_{\text{CoII}} = 1.45\mu_B$, $\mu_{\text{CoIII}} = 1.32\mu_B$, $\bar{\mu}_Y = -0.33\mu_B$, $\mu_{\text{YI}} = -0.30\mu_B$, $\mu_{\text{YII}} = -0.35\mu_B$, $\bar{\mu} = 0.92\mu_B$ for Co_3Y .

Experimentally one has $\mu_{\text{CoI}} = 1.68\mu_B$, $\mu_{\text{CoII}} = 1.67\mu_B$, $\mu_Y = -0.40\mu_B$, $\bar{\mu} = 1.33\mu_B$ for Co_5Y ; $\mu_{\text{CoI}} = 0.55\mu_B$, $\mu_{\text{CoII}} = 0.83\mu_B$, $\mu_{\text{CoIII}} = 0.40\mu_B$, $\mu_Y = -0.35\mu_B$, $\bar{\mu} = 0.33\mu_B$ for Co_3Y ; $\mu_{\text{CoI-V}} = 1.31, 1.44, 1.44, 1.34, 1.10\mu_B$, $\mu_{\text{YI}} = -1.02$, $\mu_{\text{YII}} = -0.45\mu_B$, $\bar{\mu} = 0.81\mu_B$ for Co_7Y_2 according to the magnetic neutron-scattering measurements of Krén *et al.*;²⁹ the magnetization measurements of Buschow⁷ lead to average moments of $\bar{\mu} = 1.25, 0.82$, and $0.42\mu_B$ for Co_5Y , Co_7Y_2 , and Co_3Y , respectively. The electronic structure for the Be_3Nb -type phase Co_3Y is rather different from that of the hypothetical Cu_3Au -type phase discussed by Moruzzi *et al.*¹³—this is not surprising as the local atomic arrangement is quite different. Our calculated average moments for Co_5Y is in very good agreement with the result of Coehoorn,²⁸ for Co_3Y our result is slightly higher (by $0.1\mu_B/\text{atom}$). For the Laves-phase Co_2Y at the experimental density we find a paramagnetic solution and a ferrimagnetic solution with $\mu_{\text{Co}} = 1.07\mu_B$, $\mu_Y = -0.32\mu_B$, and $\bar{\mu} = 0.61\mu_B$, depending on the initialization of the moments. This is in good agreement with the fixed-moment calculations of Mohn and Schwarz¹⁴ who found $\mu_{\text{Co}} = 1.02\mu_B$ and $\mu_Y = -0.28\mu_B$ for the ferrimagnetic solution at the equilibrium density. At this density the ferrimagnetic solution is the stable one, under

compression it becomes metastable.¹⁴ The existence of a metamagnetic state may be understood in terms of the electronic density of states: In the paramagnetic state, the Fermi level is pinned in a local minimum of the DOS, a weak spin polarization leads to an energetically less favorable situation. If the spin polarization is large enough to shift the spin-up and spin-down DOS's such that the Fermi level falls into the minima ± 0.8 eV above or below the paramagnetic E_F , this defines again a metastable solution. The metamagnetic solution appears only at the composition of the Laves phase.

Altogether the moments resulting from local-spin-density theory are slightly higher than the experimental moments, especially close to the critical concentration for the disappearance of magnetic order (see also Fig. 4). The trend to overestimate the magnetic moment

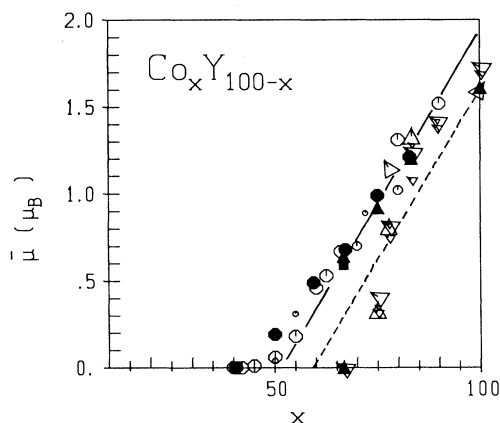


FIG. 4. Concentration dependence of the average magnetic moments in amorphous and crystalline $\text{Co}_x\text{Y}_{100-x}$: Full circles—amorphous, theory; open circles of different sizes—amorphous (expt., Refs. 3, 4, 6, and 7); full triangles—crystalline compounds, theory (present work); full squares—theory (Ref. 14), open triangles and squares—crystalline compounds, experiment (Refs. 4, 5, and 26). The straight line shows the prediction of the Friedel model assuming $\mu_{\text{Co}} = 1.64\mu_B$ (dotted line) and $\mu_{\text{Co}} = 1.9\mu_B$ (dashed line), respectively. See text.

TABLE II. Crystallographic data for the Co-Y compounds (after Ref. 24).

Compound	Structure type	Pearson symbol	Lattice constants (\AA)
Co_5Y	Cu_5Ca	$hP6$	$a = 4.942$ $c = 3.976$
Co_3Y	Be_3Nb	$hR12$	$a = 5.02$ $c = 24.40$
Co_2Y	Cu_2Mg	$cF24$	$a = 7.22$

is independent of the choice of the exchange-correlation functional (we use the Barth-Hedin form³⁰) and, in the case of the Co-based alloys, also of small changes in the atomic volume. In our opinion it is related to the well-known trend of the LSD to underestimate the equilibrium atomic volume and to the mean-field nature of LSD theory which neglects the influence of local fluctuations in the spin densities.

IV. ELECTRONIC STRUCTURE AND MAGNETIC PROPERTIES OF AMORPHOUS Co-Y ALLOYS

As for most amorphous alloys, the densities of the amorphous alloys depend somewhat on the preparation conditions (melt-spinning, sputtering, evaporation, etc.), but in general the atomic volume of the glass is rather close to that of the intermetallic compounds, as has been confirmed by detailed investigations for Ni-Y and Fe-Y. For Co-Y there are hardly any reliable density data, so we decided to model the composition dependence of the atomic volume at the example of *a*-Fe-Y, following closely the data on the intermetallic compounds as shown in Fig. 5. In principle, the equilibrium density could be calculated by minimizing the total energy versus the volume. However, as any approach based on local-density-functional theory, our method would lead to an underestimate of the atomic volume by 3–5% and this would create an ambiguity in the comparison with experiment. Hence we preferred to perform the investigations for the best available estimate of the correct density and to examine magnetovolume effects at a selected critical composition. The electronic structure has been calculated for supercells containing 64 atoms, with atomic configurations prepared by a MD quench and chosen such as to reproduce the pair correlation functions calculated for large $N = 1372$ -atom cells as closely as possible (see Refs. 10 and 11 for details). Detailed comparisons of the electronic structure of amorphous alloys calculated for 64-atom supercells with the results of real-

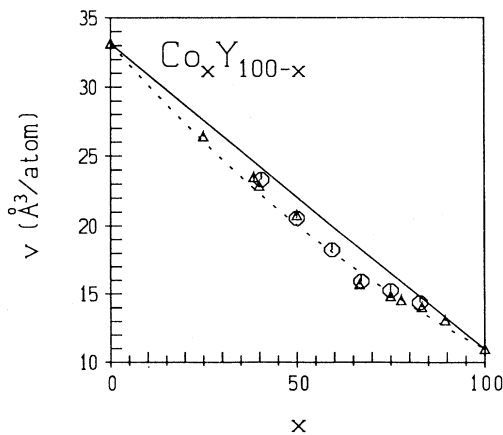


FIG. 5. Concentration dependence of the atomic volume in amorphous alloys (circles) and in crystalline intermetallic compounds (triangles).

space-recursion calculations for 800-atom ensembles using the same Hamiltonian have shown the supercell approach to be reliable.³¹

The calculated spin-polarized DOS for a series of *a*-Co_{*x*}Y_{100-*x*} alloys is shown in Fig. 6. The self-consistent calculations have been started at a very small moment for the Co atoms ($\mu_{\text{Co}} \leq 0.1\mu_B$), so that the iteration should lead to a low-spin solution—if it exists. We find that the amorphous DOS is generally a smeared-out version of the crystalline DOS, with only small changes in the bandwidth. As in the case of the crystalline intermetallic compounds, the spin-down band is usually broader and shows a more pronounced bonding-antibonding splitting than the spin-up band. The smearing effects become stronger with increased Y content. In *a*-Co₇₅Y₂₅, the DOS minimum in the minority band has nearly completely been filled up, but there are only small changes in the DOS at the Fermi level. In *a*-Co₂Y, the strongly structured DOS of the crystalline intermetallic compound has been turned into a slightly skewed rectangular *d* band. Both in the crystalline and amorphous phases, the bandwidth is approximately $W_d \sim 3.3$ eV, but the disorder-induced smearing leads to a strong increase of the DOS at the Fermi level, so that the Stoner criterion for magnetic ordering is now satisfied (note that the DOS close to E_F is dominated by the Co *d* states). Due to the disorder, the characteristic sequence of three DOS minima close to the paramagnetic Fermi level has disappeared and hence the paramagnetic solution is suppressed. This also applies to all other compositions.

The disorder-induced smearing of the DOS is caused by the breakdown of long-range translational order and not primarily by a reduction of the chemical short-range order. The reduction of the Co-Co coordination numbers with increasing Y content leads to a further narrowing of the Co 3*d* band to $W_d \sim 2.5$ eV in Co₅₀Y₅₀ and $W_d \sim 2$ eV in Co₄₀Y₆₀. The Fermi level falls at the upper edge of the *d* band and up to $x = 50$ the DOS at E_F is sufficiently high to fulfill the Stoner criterion, but from $x \sim 40$ on the Fermi level falls into a region of low DOS and the alloys are paramagnetic.

It is also interesting to have a look at the distribution of the local moments (Fig. 7). At $x = 83$ and $x = 75$, the Co moments are distributed between $1.22\mu_B \leq \mu \leq 1.75\mu_B$ and $1.19\mu_B \leq \mu \leq 1.65\mu_B$, respectively. For $x = 83$, this agrees well with the two nearly equal moments on the inequivalent Co sites in Co₅Y. For $x = 75$ the width and position of the distribution agrees well with the moments measured in crystalline Co₇Y₂ using magnetic neutron scattering,²⁹ but the moments are distinctly larger than those measured for crystalline Co₃Y. The average moments calculated for Co₇₅Y₂₅ are almost equal in the crystalline and amorphous phases. At lower Co concentrations the local Co moments show a very broad distribution, around the equiatomic composition it extends from $\mu_i = 0$ to $\mu_i \approx 1.1\mu_B$, reflecting a rather broad distribution of the number of Co-Co neighbors. The concentration variation of the calculated average moments in *a*-Co_{*x*}Y_{100-*x*} is in excellent agreement with the experimental data compiled by Buschow,⁷ Gignoux,⁴ and Malozemoff *et al.*³ (see Fig. 4). The vari-

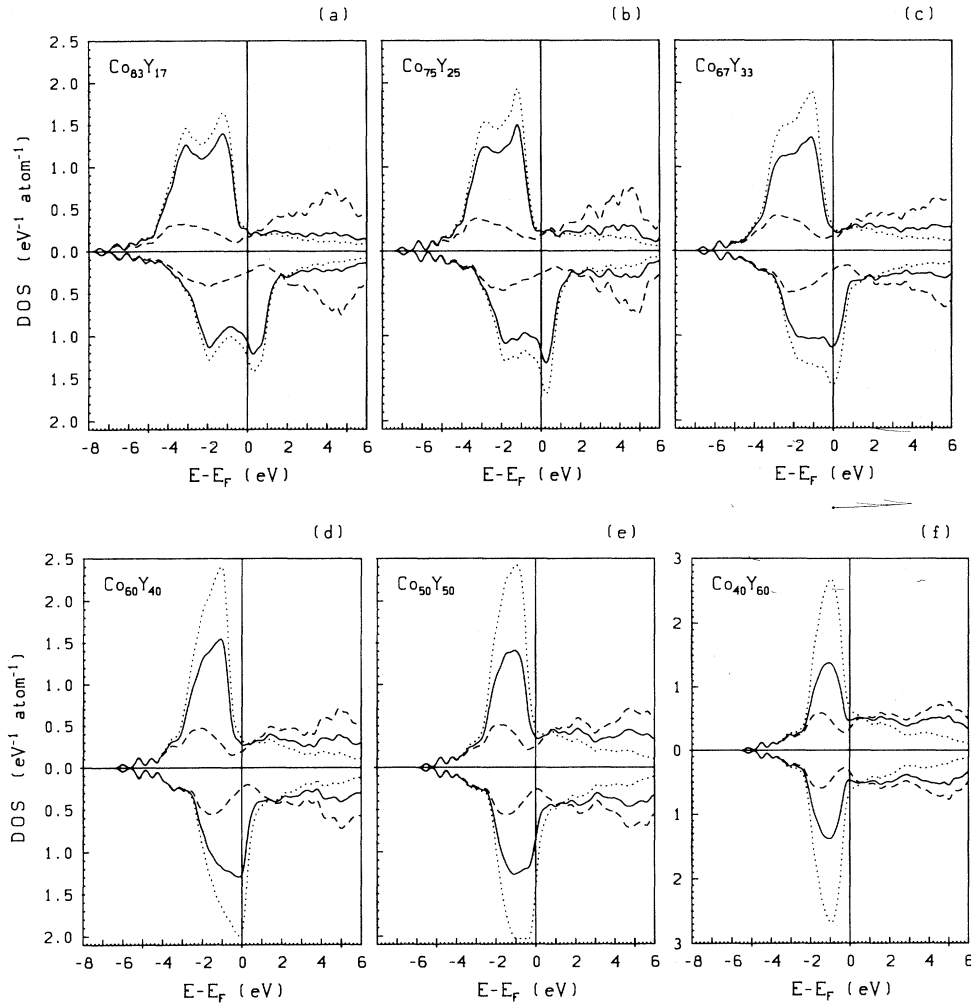


FIG. 6. Total and partial spin-polarized electronic DOS for a series of amorphous $\text{Co}_x\text{Y}_{100-x}$ alloys. Same symbols as Fig. 3.

ation of the average moment with composition is almost linear. This has sometimes been taken as an indication that the composition dependence can be explained by a simple physical mechanism.

The Friedel model³² is based on the assumption that the solute potential displaces exactly five majority electrons from below to above the Fermi level. In this case the average moment is $\bar{\mu} = \mu_0 - \frac{100-x}{100}(10 - \Delta z)$ where μ_0 is the moment of the host and Δz is the valence difference between host and solute. Here $\mu_0 = 1.64\mu_B$ and $\Delta z = 6$. In this case the disappearance of magnetic order is predicted for $x = 59$. Implicit in the Friedel model is the assumption that the density of states of the majority band is zero above E_F —this is never exactly satisfied for the pure metals. Therefore Malozemoff *et al.*³ recommended to determine an effective μ_0 by fitting the Friedel expression for $\bar{\mu}$ to the actual moments and extrapolating back to $x = 0$. This yields $\mu_0(\text{Co}) = 1.9\mu_B$ and $x_0 = 52$ and a reasonable fit to the calculated and measured average moments for $a\text{-Co}_x\text{Y}_{100-x}$ and for crystalline $\text{Co}_x\text{Y}_{100-x}$ for $x \geq 80$. This would suggest that amorphous Co-Y alloys and the Co-rich intermetallic compounds are strong ferromagnets, but that the assumption of strong ferro-

magnetism begins to break down for $c\text{-Co}_x\text{Y}$, $x = 2, 3$ where structural effects lead to an incomplete filling of the Co d band with the empty part of the band being separated from the filled part by a structure-induced gap. The strong magnetism of the amorphous alloys with a higher Y content and also of the high-spin solution of the Laves phase is confirmed by a calculation of the volume dependence of the magnetic moments in $a\text{-Co}_{67}\text{Y}_{33}$ and $c\text{-Co}_2\text{Y}$. Figure 8 shows that the distribution of the magnetic moments changes only weakly for volume changes of $\pm 10\%$ and that the moment calculated for the crystalline high-spin phase is almost equal to the average moment of the amorphous alloy.

The relation between the local atomic arrangement and the local magnetic moment has often been discussed in terms of the Jaccarino-Walker model³³ postulating that a magnetic moment is supported only on those Co sites having a minimum number of six Co neighbors. The comparison of Fig. 4 with the average coordination numbers given in Table I shows that the basic assumptions of this model do not hold for $a\text{-Co-Y}$: ferromagnetism disappears only at a composition of $\text{Co}_{40}\text{Y}_{60}$ where each Co atom has on average less than two Co neighbors as a conse-

quence of the pronounced chemical short-range order.

On the other hand it is important to emphasize the role of the ferrimagnetic coupling between the Co and Y atoms, and the strong tendency to heterocoordination. The ferrimagnetic coupling arises from the covalent coupling between the Co minority and the Y d band whose center of gravity lies at higher energies. The covalent interaction between unlike atoms is also responsible for the large bond order of the Co-Y bonds and hence for the strong CSRO. A strong CSRO with alternating Co-Y-Co ferrimagnetic bonds is equivalent to an indirect exchange interaction between the Co atoms enforcing the ferrimagnetism of the alloy. We have already emphasized the importance of this coupling mechanism in our study of α -Fe-Y alloys.

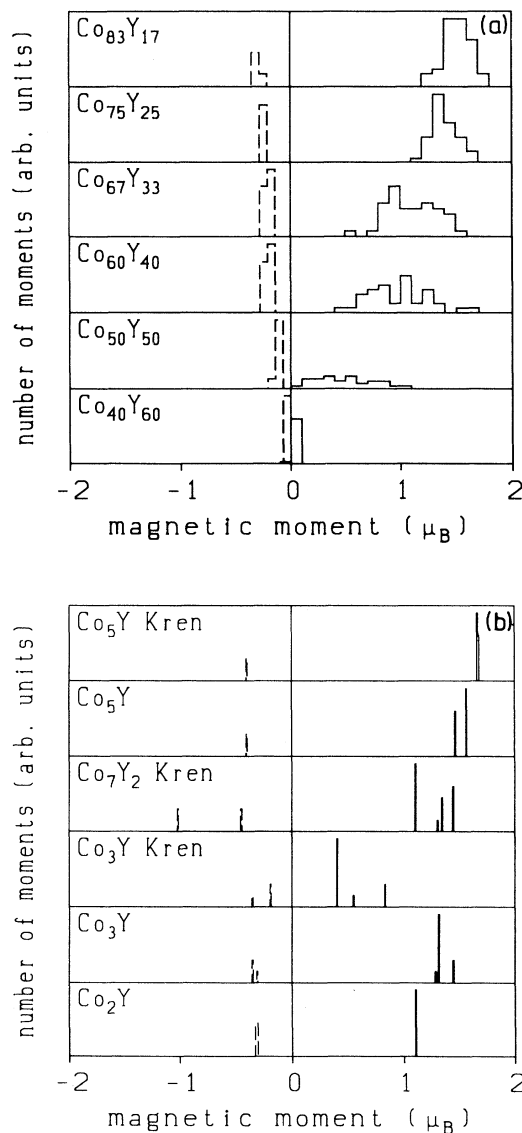


FIG. 7. Distribution of the local magnetic moments calculated for amorphous $\text{Co}_x\text{Y}_{100-x}$ (a), compared with the magnetic moments calculated for the crystalline intermetallic compounds and measured by Krén *et al.* (Ref. 29) using neutron-scattering (b).

Finally, we have also investigated the relation between the local magnetic moments μ_i and the local exchange splitting Δ_i (Fig. 9), expressed in terms of the difference in the position of the center of gravity of the local spin-up and spin-down d bands (the potential parameters $C_{d\uparrow}, C_{d\downarrow}$ of the LMTO method^{10,25}). For all individual sites in all (crystalline and amorphous) Co-Y alloys we confirm the local Stoner relation $\Delta_i = I\mu_i$ with the universal value of $I = (0.95 \pm 0.04) \text{ eV}/\mu_B$ found previously in our calculations for a large series of intertransition-metal^{10,11} and transition-metal-metalloid alloys.¹² This value also agrees with the effective Stoner parameter of

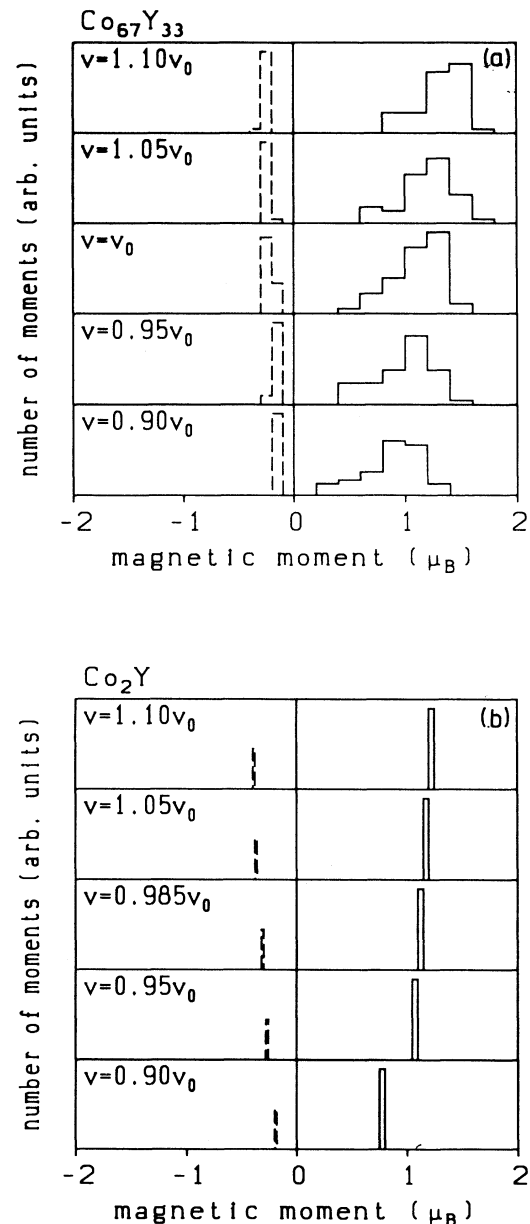


FIG. 8. Variation of the distribution of the local magnetic moments with the atomic volume in $\alpha\text{-Co}_{67}\text{Y}_{33}$ (a) and in $c\text{-Co}_2\text{Y}$ [ferrimagnetic solution (b)].

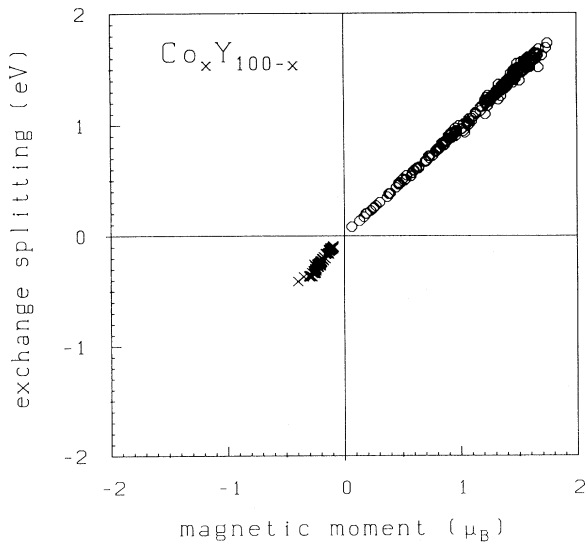


FIG. 9. Variation of the local magnetic moments μ_i with the local exchange splitting Δ_i . All sites in all amorphous alloys and crystalline intermetallic compounds have been plotted.

$I \simeq 1 \text{ eV}/\mu_B$ derived by Himpsel³⁴ from the analysis of photoemission- and inverse-photoemission spectra. It is remarkable that this relation holds equally well for the weakly magnetic Fe alloys (with asperomagnetic amorphous phases in the Fe-rich limit) and for the strongly magnetic, collinear Co-based magnets.

V. CONCLUSIONS

We have presented a detailed investigation of the structural, electronic, and magnetic properties of crystalline and amorphous Co-Y alloys. The central interest of this study lies in the investigation of the mechanism responsible for the strong enhancement of magnetism in the amorphous $\text{Co}_x\text{Y}_{100-x}$ alloys with $x \leq 75$ compared to the corresponding crystalline phases. Our calculations predict a remarkable degree of chemical and topological SRO in the amorphous Co-Y alloys which is stronger than in the α -Fe-Y, but weaker than in the α -Ni-Y alloys. The similarity of the local atomic arrangement is also reflected in the electronic densities of state: those of the amorphous phases are smeared-out versions of the crystalline DOS. Unlike for the Fe-Y alloys where the Fermi level falls close to the maximum of the paramagnetic DOS for all Y concentrations smaller than 40 at. %, in the Co-Y alloys the Fermi level falls into a region of a steeply decreasing paramagnetic DOS. In the Laves phase, the Fermi level is even pinned in a structure-induced minimum of the paramagnetic DOS. This leads to a situation where a paramagnetic solution coexists with a ferrimagnetic solution, the relative stability of the para- and ferrimagnetic solutions changing with density. In the amorphous alloys, the breaking of translational periodicity eliminates all the finer details of the crystalline DOS. The smearing leads to an increased paramagnetic DOS at E_F and hence to a larger exchange splitting and larger magnetic moments. It also eliminates the fine details of the DOS causing the

existence of a metamagnetic solution in c - Co_2Y . Independent of the density, only the high-spin solution exists in the amorphous alloys. Our argument differs to some extent from the arguments put forward by Yu and Kakehashi,¹⁶ who emphasized the importance of chemical disorder. According to these authors, nearly complete randomness (within the limits set by the size differences) would be necessary to explain the enhancement of magnetism whereas our calculations are based on models with a substantial chemical short-range order. However, in their distribution-function approach the atomic structure is characterized in a rather oversimplified way by a set of parameters such as the position and width of the nearest-neighbor peak of the pair correlation function, the partial average coordination number, etc. The values used for the parameters are based on *ad hoc* assumptions or heuristic arguments. The electronic structure too is calculated in a rather crude way. Hence the two sets of calculations are not really contradictory. Rather, our calculations could furnish the information necessary to improve the input to the distribution-function calculations whose advantage is to represent a finite-temperature theory of amorphous magnetism.

Together with our previous publications (Refs. 10–12), the present work shows that local-spin-density theory combined with modern computational techniques allows for a quantitative theory of itinerant amorphous magnets, ranging from strong, collinear ferrimagnets (like the Co-based alloys) to weakly magnetic and possibly non-collinear magnets (like the Fe-based alloys). We emphasize that the general picture emerging from these calculations is that of a pronounced similarity of the local atomic order of crystalline compounds and amorphous alloys. Any theory of the electronic and magnetic properties must start from this basic fact. The first result is the similarity of the average electronic DOS in the crystalline and amorphous phases, which differ only by a disorder-induced smearing. Hence in general the magnetic properties will be similar too. Exceptions are the Fe-rich amorphous phases where fluctuations in the *local* DOS lead to fluctuating ferro- and antiferromagnetic exchange interactions and complex spin structures,^{10–12,35} and the Co-based amorphous alloys at compositions close to and beyond the critical concentration for the disappearance of magnetism in the intermetallic compounds. Here even a modest broadening of the DOS eliminates the fine-structure responsible for the existence of metamagnetic solutions and leads to a strong increase of the DOS at the Fermi level and to enhanced magnetism. An important feature is the covalent ferrimagnetic coupling which is important for understanding the persistence of magnetic order in the Y- or Zr-rich regime.

ACKNOWLEDGMENTS

This work has been supported by the Austrian Federal Ministry for Science and Research within the Materials Research Program, Contract No. GZ 45.378/2-IV/6/94. D.S. acknowledges a leave of absence from the Department of Experimental Physics, Šafárik University, Košice (Slovakia) and financial support from the Austrian Academic Exchange Service (ÖAAD).

- ¹ K. Moorjani and J.M.D. Coey, *Magnetic Glasses* (Elsevier, Amsterdam, 1984).
- ² *The Magnetism of Amorphous Metals and Alloys*, edited by J.A. Fernandez-Baca and W.Y. Ching (World Scientific, Singapore, 1994).
- ³ A.P. Malozemoff, A.R. Williams, K. Terakura, V.L. Moruzzi, and K. Fukamichi, *J. Magn. Magn. Mater.* **35**, 192 (1983).
- ⁴ D. Gignoux, D. Givord, and A. Liénard, *J. Appl. Phys.* **53**, 2321 (1982).
- ⁵ A. Amamou, R. Kuentzler, Y. Dossmann, P. Forey, J.L. Glimois, and J.L. Ferron, *J. Phys. F* **12**, 2509 (1982).
- ⁶ N. Heiman and N. Kazama, *Phys. Rev. B* **17**, 2215 (1978).
- ⁷ K.H.J. Buschow, *J. Appl. Phys.* **53**, 7713 (1982).
- ⁸ D.H. Ryan, J.M.D. Coey, E. Batalla, Z. Altounian, and J. O. Ström-Olsen, *Phys. Rev. B* **35**, 8630 (1987).
- ⁹ J. Chappert, J.M.D. Coey, A. Liénard, and J.P. Rebouillat, *J. Phys. F* **11**, 2727 (1981).
- ¹⁰ I. Turek, Ch. Becker, and J. Hafner, *J. Phys. Condens. Matter* **4**, 7257 (1992).
- ¹¹ Ch. Becker and J. Hafner, *Phys. Rev. B* **50**, 3913 (1994).
- ¹² J. Hafner, M. Tegze, and Ch. Becker, *Phys. Rev. B* **49**, 285 (1994).
- ¹³ V.L. Moruzzi, A.R. Williams, A.P. Malozemoff, and R.J. Gambino, *Phys. Rev. B* **28**, 5511 (1983).
- ¹⁴ K. Schwarz and P. Mohn, *J. Phys. F* **14**, L129 (1984).
- ¹⁵ J. Inoue and M. Shimizu, *J. Phys. F* **15**, 1525 (1985).
- ¹⁶ Y. Kakehashi and M. Yu, *Phys. Rev. B* **49**, 15 076 (1994).
- ¹⁷ M. Maret, P. Chieux, P. Hicter, M. Atzmon, and W.L. Johnson, in *Rapidly Quenched Metals V*, edited by S. Steeb and H. Warlimont (Amsterdam, Elsevier, 1985), p. 521.
- ¹⁸ M. Maret, A. Pasturel, and P. Chieux, *J. Phys. F* **17**, 2191 (1987).
- ¹⁹ Ch. Hausleitner, M. Tegze, and J. Hafner, *J. Phys. Condens. Matter* **4**, 9557 (1992).
- ²⁰ Ch. Hausleitner and J. Hafner, *Phys. Rev. B* **45**, 115 (1992); **45**, 128 (1992).
- ²¹ Ch. Hausleitner and J. Hafner, *Phys. Rev. B* **47**, 5689 (1993); Ch. Hausleitner, J. Hafner, and Ch. Becker, *ibid.* **48**, 13 119 (1993).
- ²² J. Hafner and M. Krajčí, *J. Phys. Condens. Matter* **6**, 4631 (1994).
- ²³ J. Hafner, M. Krajčí, and M. Windisch, in *Proceedings of the 6th International Conference on the Structure of Non-crystalline Materials (NCM6)*, edited by L.Cervinka and A.C.Wright [J. Non-Cryst. Solids (to be published)].
- ²⁴ P. Villars and L.D. Calvert, *Pearson's Handbook of Crystallographic Data for Intermetallic Phases*, 2nd ed. (ASM International, Materials Park, OH, 1991).
- ²⁵ H.L. Skriver, *The LMTO Method* (Springer, Berlin, 1984); O.K. Andersen, O. Jepsen, and D. Glötzel, in *Highlights of Condensed Matter Theory*, edited by F. Bassani, F. Fumi, and M.P. Tosi (North-Holland, Amsterdam, 1985), pp. 59–176.
- ²⁶ H. Yamada, J. Inoue, K. Terao, S. Kanda, and M. Shimizu, *J. Phys. F* **14**, 1943 (1984).
- ²⁷ M. Cyrot and M. Lavagna, *J. Phys. (Paris)* **40**, 763 (1979).
- ²⁸ R. Coehoorn, *J. Magn. Magn. Mater.* **99**, 55 (1991).
- ²⁹ E. Krén, J. Schweizer, and F. Tasset, *Phys. Rev.* **186**, 479 (1969).
- ³⁰ U. von Barth and L. Hedin, *J. Phys. C* **5**, 1629 (1972).
- ³¹ S.K. Bose, S.S. Jaswal, O.K. Andersen, and J. Hafner, *Phys. Rev. B* **37**, 9955 (1988).
- ³² J. Friedel, in *Metallic Solid Solutions*, edited by J. Friedel and A. Guinier (Benjamin, New York, 1963); see also Ref. 3.
- ³³ V. Jaccarino and L.R. Walker, *Phys. Rev. Lett.* **15**, 259 (1965); see also Ref. 1.
- ³⁴ F.J. Himpsel, *Phys. Rev. Lett.* **67**, 2363 (1991).
- ³⁵ R. Lorenz and J. Hafner, *J. Magn. Magn. Mater.* **139**, 209 (1995).